Journal of Food and Drug Analysis

Volume 6 | Issue 4 Article 1

1998

Infrared Absorption Study of Schiff Bases of Aminohydroxyguanidine

Journal of Food and Drug Analysis
1998. 6(4) : 679-690

Infrared Absorption Study of Schiff Bases of Aminohydroxyguanidine

HUYNH-HOA BUI, ERIC J. LIEN* AND SHIJUN REN

Department of Pharmaceutical Sciences, School of Pharmacy, University of Southern California
1985 Zonal Ave., Los Angeles, CA 90033, U.S.A.

ABSTRACT

Schiff bases of aminohydroxyguanidine were designed to contain the essential pharmacophore of hydroxyguanidine and have structural similarity to hydroxyurea, thiosemicarbazone and N-carbamyloxyurea. Most of these compounds have been shown to have antitumor and/ or antiviral activities more potent than hydroxyurea and hydroxyguanidine. Their mode of action is inhibition of ribonucleotide reductase which is the key enzyme in *de novo* DNA synthesis. Their infrared spectra (IR) are determined and discussed in this paper. Possible applications of the IR data in pharmaceutical analysis are presented.

Key words: **infrared spectroscopy, aminohydroxyguanidines, hydroxyurea, Schiff bases.**

INTRODUCTION

Ribonucleotide Reductase is the key enzyme which catalyzes the reduction of ribonucleotides to deoxyribonucleotides in the *de novo* DNA synthesis [1]. Its activity is correlated with cell replication. This enzyme therefore is a good target for developing anticancer and antiviral agents. Hydroxyurea, hydroxyguanidine, and thiosemicarbazones are known to have antitumor and/ or antiviral activities. The mechanism of action of these compounds is the inhibition of the ribonucleotide reductase. Of these compounds, only hydroxyurea is clinically used. It has several disadvantages such as low therapeutic index, a short half life, rapid metabolic inactivation, and side effects. To optimize the anticancer and antiviral activities of ribonucleotide reductase inhibitors, Schiff bases of aminohydroxyguanidine derivatives have been developed by Lien *et al* [2,3]. These compounds were designed to contain the essential pharmacophore of hydroxyguanidine and have structural similarity to hydroxyurea, thiosemicarbazone and N-carbamyloxyurea. Fifty four substituted Schiff bases of aminohydroxyguanidine tosylate have been synthesized and tested for antitumor activities. Most of them were found to be more active than both hydroxyguanidine and hydroxyurea. Ribonucleotide reductase inhibitors can be used in combination therapy with other anticancer and antiviral drugs to reduce the chance of drug resistance [4].

In this paper, the infrared spectra of these aminohydroxyguanidine derivatives are studied.

Correspondence to: Eric J. Lien

Accepted for Publication: May 13, 1998

Although it is not possible to determine the complete structure of a compound by infrared spectrum alone, infrared spectroscopy is still one of the most useful tools in structure characterization and identification during conventional synthesis of organic compounds. It can be used in detecting the formation of new functional groups or the disappearance of a group in the starting material and in determining whether a reaction had taken place or not. Some characteristic absorption peaks of the products can be used for identification.

EXPERIMENTAL

Fifty four Schiff bases of aminohydroxyguanidine tosylate were prepared by reaction of 1-amino-3-hydroxy-guanidine with various aldehydes [5-11]. The infrared spectra were obtained as KBr pellet using a Beckman IR-4210 spectrophotometer. The absorption bands were then assigned and were in agreement with Nakanishi's and Pavia's books [12, 13].

RESULTS AND DISCUSSION

The infrared absorption frequencies of the fifty four Schiff bases of aminohydroxyguanidine derivatives are summarized in Table 1. All these derivatives contain the same aminohydroxyguanidine side-chain and the tosylate group. After Schiff base formation, all compounds show a strong absorption frequency at around 1700-1620 cm^{-1} because of the C=N stretching. The slight difference in absorption frequencies between each compound is due to the different electronic effects of different substituents. The high C=N absorption of LT5 at 1700 cm^{-1} is due to ring strain. Sulfoxide and sulfonic stretchings of the SO_3 occur between 1350-1000 cm^{-1} with two characteristic sharp peaks around 1010 cm^{-1} and 1040 cm^{-1}. The absorption peak around 1350-1300 cm^{-1} is due to the asymmetric stretching of the S=O group. The aliphatic N-C-N stretchings of the guanidine group consist of an asymmetric stretching around 1240-1200 cm^{-1} and a symmetric stretching around 980-910 cm^{-1}. C-N absorption of the aromatic ring occurs at higher frequencies around 1400-1375 cm^{-1}. Aromatic C=C absorption often occurs in pairs around 1640-1600 cm^{-1} and 1500-1450 cm^{-1}. The C=C cis alkene C=C absorption of LW02 gives a strong absorption peak at 1645 cm^{-1}. The out-of-plane C-H bending of the aromatic ring appears between 900-690 cm^{-1}. Para-substituted tosylate absorbs around 850-800 cm^{-1}. Meta-substituted rings give three absorption bands around 690 cm^{-1}, 780 cm^{-1}, and 880 cm^{-1}. Ortho-substituted rings usually have one strong band at 750 cm^{-1}. Aryl alkyl ethers show a strong asymmetric C-O-C stretching band at 1260-1200 cm^{-1} and a strong symmetric stretching around 1080-1040 cm^{-1}. The phenol groups give a C-O absorption at about 1220-1170 cm^{-1} and an O-H in-plane bending absorption at 1360-1330 cm^{-1}. The high C-O absorption frequency of the phenol is due to the conjugation of the oxygen with the ring. Aromatic NO_2 group has a strong asymmetric stretch at 1550-1530 cm^{-1} and a strong symmetric stretch at 1360-1340 cm^{-1}. The cyanide C≡N group of ATL13 has a strong absorption at 2240 cm^{-1}. The thiophene C-S has strong absorption at 730-710 cm^{-1}. The P-O stretching of the phosphonated group in LW05 occurs at 920 cm^{-1}.

Aryl bromides and iodides have absorptions between 600-550 cm^{-1}. The C-F stretching has strong absorptions at 1340-1320 cm^{-1}, 1255-1120 cm^{-1}, and 1065 cm^{-1}. Aryl chlorides absorb around 1085 cm^{-1} and 785-690 cm^{-1}. The strong C=O absorption of the amide group occur at 1740-1730 cm^{-1} in LT5 and at 1615 cm^{-1} in SRL2. The higher C=O absorption frequency in LT5 is due to the ring strain of the lactam. All compounds show a strong and broad O-H absorption between 3400-3000 cm^{-1}. The broadness of the band is due to the inter- and intramolecular hydrogen bondings. The N-H stretching occurs between 3500-3100 cm^{-1}. Aromatic C-H stretching occurs around 3200-3000 cm^{-1}, and aliphatic C-H stretching occurs between 3000-2840 cm^{-1}. The absence of the aldehlyde C-H stretching around 2775-2700 cm^{-1} along with the absence of the aldehyde C=O stretching around 1715-1695 cm^{-1} confirmed that

Table 1. Infrared absorption frequencies

R-CH=N-NH-C (=NH) NHOH. H_3C— 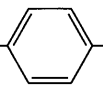 —SO_3H

Absorption in Wavenumbers (cm^{-1})

Compound R-	vC-H		vC=N	vN-H	vO-H	vC-N		vC=C	vS=O	Arom subst	Other
	arom	aliph				aliph	arom				
ATL11 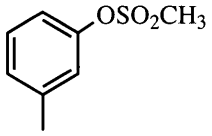	3060-3000 (b,w)	2940-2880 (b,w)	1670 (s)	3240 (b,w) 3180-3160 (b,w)	3390 (b,w)	1230 (b,w) 970 (s)		1630(s) 1600(m) 1485(m) 1425(w)	1360(s) 1180(s) 1120(s) 1030(s) 1010(s)	680(s) 890(m) 820(s) 790(w)	
ATL12 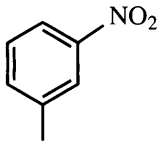	3000 (w)	2830 (w)	1670 (s)	3220 (b,w) 3160 (b,m)	3360 (b,m)	1230 (b,s) 960 (s)		1630(s) 1485(m) 1450(m)	1300(w) 1130(b,s) 1155(b,s) 1015(s) 1040(s) 1015(s)	680(s) 775(w) 895(m) 825(s)	vNO_2 1530(s) 1360(s)
ATL13 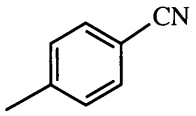	3000 (b,w)	2860 (b,w)	1670 (s)	3230 (b,w) 3170 (b,m)	3370 (b,m)	1235 (b,s) 975 (m)		1640(s) 1600(w) 1500(m) 1460(b,w)	1350(m) 1150(b,s) 1130(b,s) 1040(s) 1015(s)	830(s)	vC=N 2240(s)
ATL14 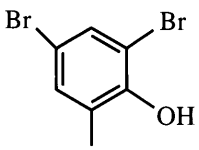	3080-2940 (b)	2860 (w)	1670 (s)	3230 (w) 3260(b) 3180-3160 (m)	3340 (b,w)	1225 (b,s) 970 (m) 925 (b,m)		1640(s) 1600(w) 1500(b,w) 1460(m)	1350(m) 1150(b,s) 1125(w) 1040(s) 1015(s)	880(s) 820(s)	vC-Br 560(m) vC-O 1070(m)
ATL15 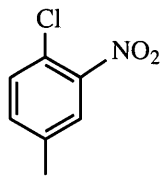	3000 (w)	2860 (w)	1670 (s)	3230 (b,w) 3180 (b,m)	3370 (b,w)	1230 (b,s) 960 (m)		1640(s) 1600(w) 1490(m) 1455(b,m)	1300(m) 1150(b,s) 1130(b,s) 1040(s) 1015(s)	890(s) 850(s) 830(s)	vC-Cl 760(m) 780(b,w) 1085(b,m) vNO_2 1540(s) 1365(s)
ATL16 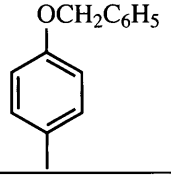	3200 (b,m) 3020 (w)	2890 (w) 2870 (w)	1670 (s)	3400 (b,w) 3340 (w)	3490 (m)	1210 (m) 970 (w)		1635(b,s) 1610(m) 1520(s) 1465(b,m)	1320(m) 1150(m) 1130(m) 1040(s)	690(s) 750(s) 820(s) 830(s)	vC-O 1260(m) 1090(w)

Table 1. Continued

Compound R-	νC-H		νC=N	νN-H	νO-H	νC-N		νC=C	νS=O	Arom subst	Other
	arom	aliph				aliph	arom				
		2835 (w)							1020(s)		
ATL17 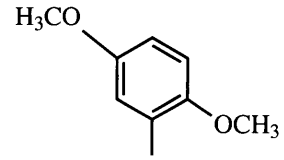	3020 (w) 2980 (w)	2960-2920 (b,m)	1680-1655 (b,m)	3260 (b,w) 3180(b)	3460 (b,w)	1230 (m) 960 (m)		1630(b,s) 1500(s) 1470(b,m)	1350(m) 1150(w) 1130(w) 1080(s) 1015(s)	875(w) 810(m)	νC-O 1270(m) 1290(m) 1040(s)
ATL18 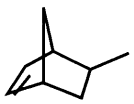	3020 (b,w) 2980 (b,m)	2950-2880 (b,w)	1680 (s)	3260 (w) 3180 (b,m)	3450 (b,m)	1210 (w) 960 (w)		1600(s) 1500(w) 1465(b,m) 1450(w)	1350(s) 1135(m) 1040(s) 1020(s)	820(s)	δC-H 690(s)
ATL19 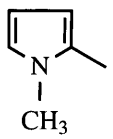	3170 (b)	2960 (w) 2870 (w)	1675 (s)	3260-3220(b)	3440 (s)	1205 (w) 950 (m)		1635(s) 1470(m) 1445(m)	1130(b) 1035(s) 1010(s)	810(s) 725(s)	νC-N 1305(s)
ATL21 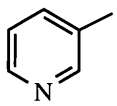	3030 (b,w) 2990 (b,w)	2890 (b,w)	1670 (b,s)	3200-3100(b)	3350 (b,m)	1200 (b,w) 970 (m)	1380 (b,m)	1630(m) 1610(m) 1480(s) 1430(s)	1325(m) 1145(b,m) 1120(b,m) 1035(s) 1010(s)	815(s) 750(m)	
ATL24 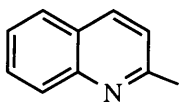	3050 (w)	2930 (b,w)	1680 (s)	3200-3120 (b,w)	3350 (b,w)	1225 (s) 940 (s)	1375 (s)	1625(b,s) 1600(s) 1510(s) 1460(b,m)	1310(m) 1155(b,s) 1130(m) 1040(s) 1010(s)	830(s) 825(s) 760(s)	
ATL25 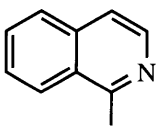	3120-3020 (b,s) 3030 (b,w) 3010 (b,w)	2870 (b,m)	1675 (s)	3230 (b,w) 3180 (b,w) 3400 (b,s)	3490 (m)	1215 (b,s) 945 (m)	1395 (s)	1630(s) 1600(s) 1500(w) 1460(b,m)	1325(s) 1130(b,s) 1040(s) 1015(s)	830(s) 815(s) 750(s)	νC-N 1565(s) 1510(w)
ATL26	3070 (b,w)	2980-2920	1665 (s)	3240-3220	3380 (b,w)	1230-1220		1630(b,m)-1610(m)	1340(s) 1150-	825(s)	νC-F 680(s)

Table 1. Continued

Compound	R-	νC-H		νC=N	νN-H	νO-H	νC-N		νC=C	νS=O	Arom subst	Other
		arom	aliph				aliph	arom				
	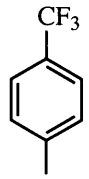		(b,w)		(b,w) 3160-3150 (b,w)		(b,w) 970 (s)		1500(m) 1450(b,m)	1120(b,w) 1040(s) 1010(s)		765(b,m) 1170(s)
LT1	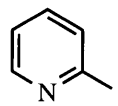	3080 (b)	2950-2800 (b)	1670 (s)	3240-3120(b)	3375 (s)	1240 (s) 960 (s)	1245 (s)	1630-1590(s) 1475-1450(m)	1160-1105(b) 1035(s) 1015(s)	820(m) 750(m) 685(s)	
LT2	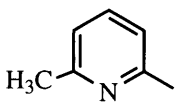	3010 (b)	2980-2840 (b)	1680 (s)	3220-3060(b)	3310 (b)	1215 (s) 940 (s)		1610-1570(b) 1460(s)	1170 1125(s) 1040(s) 1010(s)	820 810(m) 740(m) 680(b)	
LT3	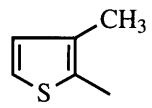	3100 (b)	2990-2840 (b)	1660 (s)	3380-3040(b) -	3415 (b)	1200 (b) 930 (m) 950 (m)		1630(b) 1425(b)	1160-1120(b) 1035(s) 1010(s)	820 815(m) 685(b)	νC-S 720(m)
LT4	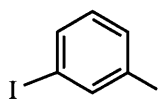	3000 (b)	2950	1660 (s)	3260-3070(b)	3360 (s)	1235 (m) 1215 (m) 955 (s)		1630(s) 1480-1450(m)	1150(s) 1125(s) 1035(s) 1010(s)	820(s) 780(s) 680(s)	νC-I 600-550(s)
LT5[a]	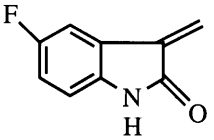	3010 (b)	2970-2860	1700 (s)	3240-3040(b)	3300 (b)	1488 (s) 930 (m)		1620(b) 1570(b) 1488(s)	1170-1120(s) 1040(s) 1015(s)	820 760(m) 685(b)	νC=O 1740-1730 νC-F 1130(s)
LT6	H_2	3120 (b)	2920 (b)	1690 (s)	3360-3080(b)	3500 (s)	1200 (b) 940 (s)		1650(b) 1490(m)	1160-1120(b) 1035(s) 1010(s)	820 815(s) 685(b)	
LT7		3040	2950-	1670	3320-	3400	1215		1630(b)	1160-	820(m)	νC-O

Table 1. Continued

Compound	R-	νC-H		νC=N	νN-H	νO-H	νC-N		νC=C	νS=O	Arom subst	Other
		arom	aliph				aliph	arom				
	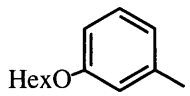	(b)	2850 (m)	(s)	3100(b)	(b)	(b) 945 (s)		1590(s) 1490(s)	1130(b) 1040(s) 1015(s)	790(s) 685(s)	1265(s)
LT8	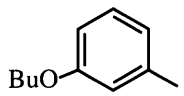	3025 (b)	2960-2880 (m)	1680 (s)	3100-3340(b)	3420 (b)	1220 (b) 950 (s)		1630(b) 1600(s) 1495(m)	1170-1130(b) 1190(b) 1165(b) 1040(s) 1015(s)	820(m) 745(w) 795(s) 690(s)	νC-O 1275-1265
LT9	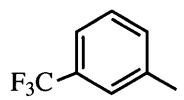	3020 (w)	2995-2850 (b)	1660 (s)	3220(b) 3160(b)	3360 (s)	1212 (s) 955 (m)		1630(s) 1490(w) 1450(w)	1170-1120(s) 1035(s) 1010(s)	820(m) 805(m) 770(b) 690(s)	νCF_3 1120 1175-1150 1340-1320
LT10	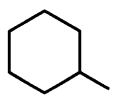	3020 (m)	2990-2860 (m)	1660 (s)	3220(b) 3180(s)	3360 (s)	1215 (s) 1235 (s) 960 (m)		1630(s) 1495(w) 1450(w)	1170-1130(s) 1040(s) 1015(s)	822(m) 810(m) 775(b) 690(s)	νCH_2 1455
LT11	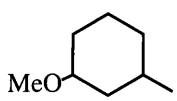	3020 (w)	2970-2840 (b)	1675 (s)	3370 (m) 3175(s)	3445 (b)	1205 (s) 950 (m)		1645(s) 1610(m) 1495(m) 1460(m)	1170-1130(s) 1040(s) 1015(s)	820(s) 780(m) 685(m)	νC-O 1300-1275 1040
LT12	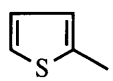	3040 (w)	2990-2880 (b)	1670 (s)	3350-3080(b)	3440 (s)	1210 (s) 935 (s)		1630(s) 1495(m) 1435(s)	1170-1130(s) 1040(s) 1015(s)	820(s) 775(w) 690(s)	νC-S 730-710(s)
LW01	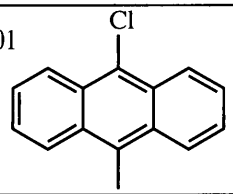	3080-3020 (b,w)	3000-2900 (b,w)	1640 (s)	3360-3100 (b,s)	3460 (w)	1280 (s) 960 (m)		1600(m) 1550(s) 1500(w) 1450(s)	1350(s) 1170(s) 1040(sh) 1020(sh)	820(s)	νC-Cl 690(s)
LW02	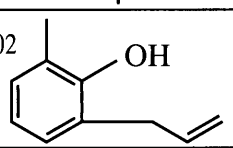	3090 3020 (b,w)	2920-2840 (w)	1680 (s)	3250-3100 (b,s)	3380 (w)	1290 (s) 980		1660(m) 1500(w) 1470(s)	1310(s) 1150(w) 1040(sh)	830(s) 750(s) 710(m)	$\nu CH_2=CH_2$ 1645(s) νC-O

Table 1. Continued

Compound R-	νC-H		νC=N	νN-H	νO-H	νC-N		νC=C	νS=O	Arom subst	Other
	arom	aliph				aliph	arom				
						(s)		1430(sh)	1020(sh)		1240-1200 (b,s) δO-H 1350(m)
LW03 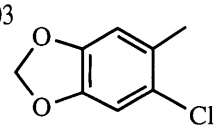	3080-3082 (b,w)	2920-2910 (w)	1680 (s)	3230-3160 (b,m)	3370 (m)	1260 (sh) 940 (m)		1640(s) 1510(s) 1480 (s,sh) 1430(sh)	1150(sh) 1130(sh) 1040(sh) 1020(sh)	850(m) 820(m)	νC-Cl 690(s) νC-O 1200(m) 1050(w)
LW04 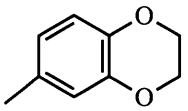	3060-3020 (b,w)	2930-2840 (b,m)	1680 (s)	3280-3120 (b,m)	3340 (m)	1260 (sh) 930(s)		1590 (sh) 1520(s)	1310(sh) 1150(s) 1120(s) 1030(sh) 1010(sh)	825(s) 750(w)	νC-O 1240(m) 1070(s)
LW05 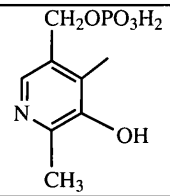	3080 (w)	2900-2860 (b,w)	1640 (s)	3210-3120 (b,w)	3360 (w)	1260 (w) 950 (m)	1390 (s)	1575(s) 1520(m)	1130(s) 1100(s) 1040(s) 1020(sh)	820(s) 750 (w) 700(s)	νP-O 920(sh) δO-H 1350(b,w)
LW06 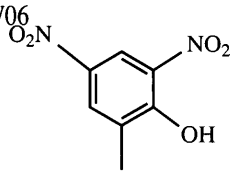	3100 (w)	2940-2910 (b,w)	1640 (s)	3340-3160 (b,m)	3420 (w)	1270 (sh) 960 (m)		1600(w) 1490(w) 1450(s)	1170(w) 1130(w) 1040(sh) 1020(sh)	820(s) 780(sh)	νNO_2 1550(sh) 1340(sh)
LW07 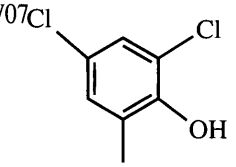	3090 (w)	2880 (w)	1670 (s)	3240-3120 (b,m)	3340 (m)	1240 (s) 970 (s)		1640(sh) 1610(s) 1470(s)	1150(s) 1110(sh) 1040(sh) 1020(sh)	825(s) 750(w)	νC-Cl 690(sh) δO-H 1350(w)
LW08 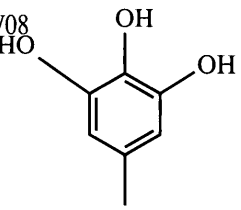	3080-3020 (w)	2910 (w)	1670 (s)		3450-3100 (b,s)	1300 (s) 970 (s)		1640(s) 1600(s) 1440(s)	1130(s) 1040(sh) 1020(sh)	850(m) 810(s)	νC-O 1220-1170(b) δO-H 1340(b,m)
LW09	3080 (w)	2940 (m)	1680 (s)	3360-3150 (b,s)	3500 (sh)	1280 (s) 970		1640(s) 1600(m) 1520(m)	1140(b) 1040(sh) 1020(sh)	810(s)	νC-O 1180(s) δO-H

Table 1. Continued

Compound	R-	νC-H arom	νC-H aliph	νC=N	νN-H	νO-H	νC-N aliph	νC-N arom	νC=C	νS=O	Arom subst	Other
	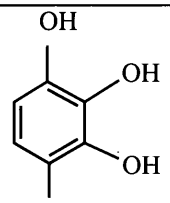						(m)		1490(m)			1340(s)
LW10	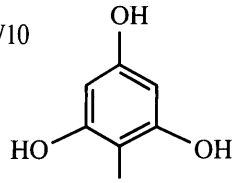	3010 (w)	2910 (w)	1640 (s)	3370-3100 (b,m)	3420 (w)	1270 (w)		1600(w) 1470(s)	1040(sh) 1020(sh)	810(s)	νC-O 1210(b) δO-H 1330(m)
LW11	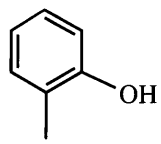	3080-3040 (b,w)	2940-2850 (b,w)	1640 (s)		3500-3100 (b,m)	1280 (sh)		1600(w) 1520(m) 1460(m)	1320(sh) 1170(m) 1130(m) 1020(sh) 1040(sh)	890(s) 820(s) 805(s)	νC-O 1220(b) δO-H 1360(s)
LW12	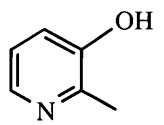	3080-3060 (w)	2880-2860 (w)	1680 (m)	3310-3110 (b,m)	3380 (w)	1280 (sh) 965 (m)	1390 (w)	1640(s) 1620(w) 1490(sh) 1450(w)	1170(w) 1090(b) 1040(sh) 1020(sh)	820(s) 790(s) 750(s)	νC-O 1220(b) δO-H 1360(sh)
ML1	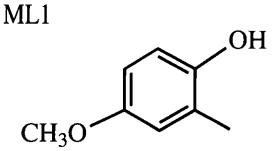	3220-3040 (m)	3040-3000 (w)	1680 (s)	3320-3220 (m)	3350 (w) 3370 (w)	1270 (s) 960 (m)		1640(s) 1580(w) 1500(s)	1170(m) 1120(m) 1040(s) 1010(s)	805(s) 770(m)	νC-O 1210(s) 1050(m) δO-H 1350(m)
ML2	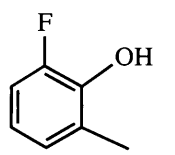	3220-3120 (m)	3040-2980 (w)	1670 (s)	3220 (w)	3340 (m)	1270 (m) 970 (m)		1640(s) 1485(s)	1140(m) 1120(m) 1040(s) 1010(s)	810(s) 770(s) 720(s)	νC-F 1065(m) νC-O 1210(s) δO-H 1350(m)
ML3	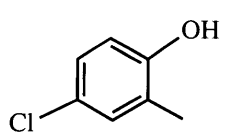	3220-3040 (m)	3040-2980 (w)	1680 (s)	3230 (w)	3320 (w)	1270 (s) 960 (w)		1635(s) 1480(s)	1160(s) 1120(s) 1030(s) 1005(s)	810(s)	νC-Cl 780(m) νC-O 1210(s) δO-H 1350(m)

Table 1. Continued

Compound R-	νC-H		νC=N	νN-H	νO-H	νC-N		νC=C	νS=O	Arom subst	Other
	arom	aliph				aliph	arom				
ML4 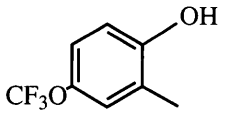	3210-3105 (b)	2940-2920 (w)	1670 (s)	3230 (w)	3330 (w)	1260 (s) 965 (s)		1640(s) 1490(s)	1160(s) 1120(s) 1030(s) 1005(s)	810(s)	νC-F 1255(s) νC-O 1210(s) δO-H 1350(m)
ML10 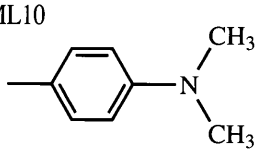	3220-3060 (b)	3000-2960 (w)	1660 (s)	3240 (w)	3360 (w)	1180 (m) 950(s)		1630(s) 1600(s) 1520(s)	1140(w) 1120(m) 1030(s) 1005(s)	810(s)	δC-H 1360(s)
ML12 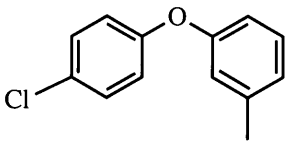	3220-3060 (b)	2940-2860 (b)	1665 (s)	3250 (w)	3340 (b,m)	1215 (m) 945 (m)		1635(s) 1600(s) 1485(s)	1160(w) 1120(m) 1030(s) 1005(s)	835(s) 805(s)	νC-Cl 785(m) νC-O 1250(s) 1080(m)
LK02 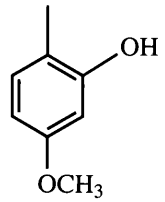	3220-3180 (b,w)	3020 (b)	1680 (s)	3240 (b,w)	3390 (b,w)	1230 (b,w) 970 (s)		1470-1450 (b,w)	1350(s) 1180(s) 1120(s) 1050(s) 1020(s)		
LK03 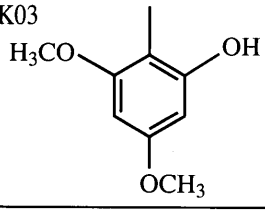	3210-3160 (b,w)	2910-2880 (b,w)	1630 (s)	3240 (b,w)	3390 (sh, m)	1220 (b)		1480-1430 (b,w)	1350(s) 1180(s) 1120(s) 1050(s) 1020(s)		
LK04 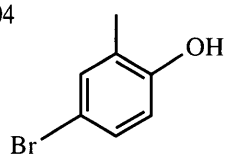	3200-3100 (b,w)	2860-2840 (b,w)	1680 (s)	3240 (b,w)	3380 (b,w)	1260 (s) 960 (s)		1640 (b,w) 1480(s)	1340(s) 1160(b) 1120(s) 1030(s) 1000(s)		νC-Br 550(b,m)
LK05 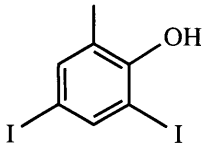	3200-3150 (b,w)	2900-2852 (b,w)	1660 (s,m)	3240 (b,w)	3320 (b,w)	1270 (s) 960 (s)		1620 (b,w) 1440(s)	1340(s) 1160(b) 1120(s) 1030(s) 1005(s)		νC-I 550(b,m)

Table 1. Continued

Compound R-	νC-H		νC=N	νN-H	νO-H	νC-N		νC=C	νS=O	Arom subst	Other
	arom	aliph				aliph	arom				
LK06 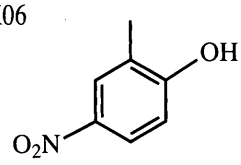	3200-3150 (b,w)	2910 (b)	1650 (s)	3240 (b,w)	3400-3300 (b,w)	1270 (s) 960 (s)		1620 (m,sh) 1420(w)	1340(s) 1160(s) 1120(s) 1010(s) 1040(s)		νNO2 1530(m) 1360(s)
LK07 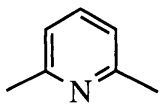	3200-3190 (b,w)	2920-2910 (b,w)	1680 (s)	3240 (b,w)	3360 (sh, m)	1290 (s) 950 (sh, w)		1600 (m,sh) 1480 (m,sh)	1340(s) 1170(s) 1120(s) 1040(s) 1070(s)		
LK10 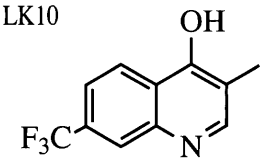	3250-3150 (b,w)	2960 (b,w)	1620 (s)	3180 (b,w)	3340 (b,w)	1260 (w) 910 (s)		1560(m) 1480(s)	1360(s) 1160(b) 1120(b) 1030(s) 1010(s)		νC-F 680(s) 760(s)
LK11 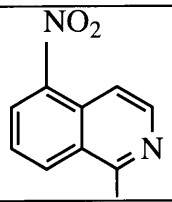	3250-3150 (b,w)	2840 (b,w)	1670 (s)	3140 (b,w)	3400-3300 (b,w)	1350 (m) 910 (s)		1520(w) 1460(w)	1120(s) 1030(s) 1010(s)		νNO_2 1530(m) 1360(s)
ADL1[b] 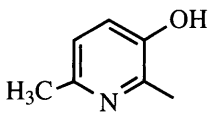	3060-2930 (b,w)	2870 (m)	1685 (sh,s)	3220-3060 (b,m)	3560-2600 (b,s)	1240 (b) 930 (w)	1400 (b,w)	1600(s) 1545(s) 1497(m) 1450(m)	1325 (sh,m) 1175(s,b) 1120(b,s) 1030(s,sh) 1005(s,sh)	820 (m)	δN-H 1642(m) 630(w) νC-O 1265(sh)
ADL2 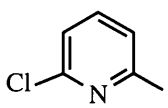	3020 (w) 2920 (w)	2860 (w)	1670 (sh,s)	3250-3220 (m)	3380-2900 (b,s)	1205 (s) 945 (m)	1390 (sh, m)	1575(sh) 1550(sh) 1489(m) 1430 (sh,s)	1320(m) 1160(s,sh) 1125(sh) 1030(s,sh) 1005(s,sh)	795 (sh,m)	δN-H 1640(sh) 620(b,m) νC-Cl 730(w)
SRL2 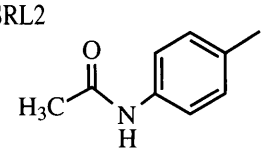	3000 (w)	2995 (m) 2850 (m)	1665 (s)	3350 (s)	3320-3010 (b)	1210 (s) 930 (w)	1270 (sh,s)	1545(s) 1510(s) 1445(m) 1405(s)	1325(s) 1148(s) 1115(s) 1025(s) 1002(s)	800 (b,s)	δN-H 1595(s) 630(b) νC=O 1615(b,s)

s = strong, m = medium, w = weak, sh = sharp, b = broad.

[a] R=N-NH-C(=NH)NHOH . H_3C-C_6H_4-SO_3H.

[b] R-CH=N-NH-C(=NH)NHOH . $2H_2O$. 1.94 H_3C-C_6H_4-SO_3H. This stoichiometric ratio was confirmed by mass spectroscopy using electronspray ionization [14].

Schiff base formation had taken place.

CONCLUSION

The infrared spectra of these 54 Schiff bases confirmed the structures identified by NMR, elemental analysis and other means. The specific absorption peaks can be used for future characterization and identification of new compounds resulting from combinatorial or conventional synthesis of related compounds (e.g. aminohydroxyguanidines, aminohydroxyureas, etc.). In some cases, infrared spectroscopy can be used to detect the presence of moisture or other impurities, the presence or absence of ring strain, intramolecular or intermolecular hydrogen bonds and the different degrees of inductive effect caused by various substituent groups [15].

REFERENCES

1. Cory, J. G., Carter, G. L., Bacon, P. E., T'ang, A. and Lien, E. J. 1985. Inhibition of ribonucleotide reductase and L1210 cell growth by N-hydroxy-N'-aminoguanidine derivatives. Biochem. Pharmacol. 34: 2645-2650.
2. Lien, E. J. 1987. Ribonucleotide reductase inhibitors as anticancer and antiviral agents. Prog. Drug. Res. 31: 101-126.
3. Lien, E. J. 1987. Chapter 4. Ribonucleotide reductase inhibitors as antiviral and anticancer agents. In "SAR: Side Effects and Drug Design". pp. 163-182. Marcel Dekker, Inc., New York, U.S.A.
4. Ren, S. and Lien, E. J. 1998. Development of HIV protease inhibitors: A survey. Prog. Drug. Res. 51: 1-30.
5. Das, A. 1996. Antiviral Activities and Cytotoxicities of Heterocyclic Schiff Bases of Aminohydroxyguanidine. Ph. D. Dissertation. pp. 1-133. University of Southern California, Los Angeles.
6. Hui, M. B. V. 1992. Development of New Substituted Schiff Bases of Aminohydroxyguanidine as Antiadenoviral Agents. Ph. D. Dissertation. pp. 1-131. University of Southern California, Los Angeles.
7. Koneru, P. B. 1992. Improvement of Antileukemic Activity of Hydroxyaminoguanidine Derivatives by Molecular Modification and through Combination with Cytarabine against CCRF-CEM/0 Cells. Ph. D. Dissertation. pp. 1-225. University of Southern California, Los Angeles.
8. Tai, A. W. 1982. Design of Novel 1-Amino-3-Hydroxyguanidine Derivatives as Antiviral and Anticancer Agents. Ph. D. Dissertation. pp. 1-170. University of Southern California. Los Angeles.
9. T'ang, A. 1984. Optimization of Ribonucleotide Reductase Inhibitors as Anticancer and Antiviral Agents: N-Hydroxy-N'-Aminoguanidine Derivatives. Ph. D. Dissertation. pp. 1-204. University of Southern California. Los Angeles.
10. Wang, P. 1989. Design, Synthesis, Testing and QSAR Analysis of Substituted Salicylaldehyde Schiff-bases of 1-Amino-3-hydroxyguanidine Tosylate as New Antiviral Agents Against Coronavirus. Ph. D. Dissertation. pp. 1-162. University of Southern California. Los Angeles.
11. Ren, S. 1997. Unpublished results. University of Southern California. Los Angeles.
12. Nakanishi, K. and Solomon, P. H. 1977. Infrared Absorption Spectroscopy. 2nd ed. pp. 1-287. Holden-Day, Inc., Oakland, U.S.A.
13. Pavia, D. L., Lampman, G. M. and Kriz, G. S. 1996. Introduction to Spectroscopy. pp. 14-95. Saunders College Publishing, Florida, U.S.A.

14. Das, A., Lien, E. J. and Trousdale, M. D. 1997. Synthesis and antiviral activities of heterocyclic Schiff bases of aminohydroxyguanidine. Chin. Pharm. J. 49: 89-102.

15. Lien, E. J. and Gao, H. 1995. New applications of spectroscopic methods in biomedical and pharmaceutical analysis: A survey. Journal of Food and Drug Analysis 3: 1-16.

氨基羥基胍（Aminohydroxyguanidine）西佛鹼（Schiff Bases）之紅外光譜吸收研究

裴黃花　連榮吉*　任士君

南加州大學藥學院

摘　要

氨基羥基胍的西佛鹼衍生物具有羥基胍藥效團，其結構與羥基脲，縮氨基硫脲和甲氨酰脲類似，實驗證明這類化合物多數具有比羥基脲及羥基胍更強的抗腫瘤和／或抗病毒活性。這類化合物的作用機制是抑制DNA合成的關鍵酶—核糖核苷酸還原酶。這篇論文研究並討論了54個這類化合物的紅外光譜及其在藥物分析中可能的應用。

關鍵詞：紅外光譜，氨基羥基胍，羥基脲，西佛鹼。